Taylor & Francis
Taylor & Francis Group

Journal of Toxicology and Environmental Health, Part A
Current Issues

ISSN: 1528-7394 (Print) 1087-2620 (Online) Journal homepage: https://www.tandfonline.com/loi/uteh20

Modifications of carbon black nanoparticle surfaces modulate type II pneumocyte homoeostasis

Nicole Schreiber, Michael Ströbele, Renate Hochscheid, Elke Kotte, Petra Weber, Henning Bockhorn & Bernd Müller

To cite this article: Nicole Schreiber, Michael Ströbele, Renate Hochscheid, Elke Kotte, Petra Weber, Henning Bockhorn & Bernd Müller (2016) Modifications of carbon black nanoparticle surfaces modulate type II pneumocyte homoeostasis, Journal of Toxicology and Environmental Health, Part A, 79:4, 153-164, DOI: 10.1080/15287394.2015.1124819

To link to this article: https://doi.org/10.1080/15287394.2015.1124819

JOURNAL OF TOXICOLOGY AND ENVIRONMENTAL HEALTH, PART A
2016, VOL. 79, NO. 4, 153–164
http://dx.doi.org/10.1080/15287394.2015.1124819

Taylor & Francis
Taylor & Francis Group

Modifications of carbon black nanoparticle surfaces modulate type II pneumocyte homoeostasis

Nicole Schreiber[a], Michael Ströbele[b], Renate Hochscheid[a], Elke Kotte[a], Petra Weber[a], Henning Bockhorn[b], and Bernd Müller[a]

[a]Laboratory of Respiratory Cell Biology, Division of Pneumology, Faculty of Medicine, Philipps University, Marburg, Germany; [b]Karlsruhe Institute of Technology, KIT Campus South, Engler-Bunte-Institute, Karlsruhe, Germany

ABSTRACT

Inhalation uptake of carbon black nanoparticles (CBNP) bears the risk of morphological and functional lung impairment attributed to the highly reactive particle surface area. Chemical particle surface modifications might affect particle–cell interactions; however, thus far these alterations have not been determined. This is the first in vivo study comparing particle-induced acute lung injury using Printex®90 (Pr90, 7 µg), Printex®90 covered by benzo[a]pyrene or 9-nitroanthracene (BaP-Pr90, NA-Pr90, 7 µg, 15% BaP or NA by weight), and acetylene carbon black (CB) with polycyclic aromatic hydrocarbons (PAH-AB, 7 µg, 20% PAH by weight). All particles were suspended in distilled water with bovine serum albumin (BSA). In addition, the influence of suspension media was tested using Printex®90 suspended without BSA ($Pr90^{-BSA}$, 7 µg). Quartz (DQ12, 7 µg), 70 µl saline (NaCl), and distilled water with or without BSA ($H_2O^{+/-BSA}$) were used as reference and controls. It was postulated that CBNP surface modifications trigger pulmonary responses. After oropharyngeal particle aspiration, lung functions were measured 2 d postexposure, followed by lung preparation for histological or bronchoalveolar lavage fluid (BALF) examinations and type II pneumocyte isolation on d 3. Head-out body plethysmography revealed reduced flow rates induced by PAH-AB. Examinations of BALF demonstrated reduced influx of macrophages after exposure to $Pr90^{-BSA}$ and decreased lymphocyte levels after $Pr90^{+BSA}$ or BaP-Pr90 treatment. Further, CBNP induced changes in mRNA expressions (surfactant proteins) in type II pneumocytes. These findings indicate that CBNP surface area and media modulate interactions between NP and lung cells in short-term experiments.

ARTICLE HISTORY
Received 2 July 2015
Accepted 23 November 2015.

Carbon black nanoparticles (CBNP) are characterized by a defined size, chemical composition, surface area, and specific surface modifications such as functional groups (Long et al., 2013). The use of CBNP in rubber tire, lacquer, and printing ink industries is rising continuously (Ceresana, 2014). However, the toxic potential of different CBNP surface modifications is still unknown. It was postulated that specific surface modifications trigger responses differently in the terminal respiratory tract.

During the last decades a number of investigations on CBNP interactions with tissues and organ systems were conducted (Shimada et al., 2006; Nassimi et al., 2010; Kim et al., 2012; Saber et al., 2013; Han et al., 2015) showing that unmodified CBNP in varying doses and at varying exposure durations have potential to impair structural and functional lung integrity (Renwick et al., 2004; Niwa et al., 2008; Bourdon et al., 2013; Schreiber et al., 2013). With regard to possible adverse health effects attributed to CBNP (International Agency for Research on Cancer [IARC]/World Health Organization [WHO], 2010), chemical surface modification is considered to be a factor to influence the actions of CBNP.

To the best of our knowledge the influence of surface-modified carbon-based nanomaterials on lungs is less investigated. To date, only studies with surface-modified single- (SWCNT) and multi-walled carbon nanotubes (MWCNT) were conducted to improve their biocompatibility, because they are potential therapeutic agents (Sayes et al., 2006; Dumortier et al., 2006; Yu et al., 2013). Saber and colleagues (2012) investigated the inflammatory

CONTACT Nicole Schreiber nicole.schreiber@staff.uni-marburg.de Laboratory of Respiratory Cell Biology, Division of Pneumology, Faculty of Medicine, Philipps University, Baldingerstrasse, 35043 Marburg, Germany.

Color versions of one or more of the figures in the article can be found online at www.tandfonline.com/uteh

and genotoxic potential of titanium dioxide (TiO_2) that was either uncoated or coated with silicon, aluminum, zirconium and polyalcohol, or aluminum and polyalcohol and compared to the reference Printex®90. All particles were intratracheally (IT) instilled to mice and for 24 h. Printex®90 and uncoated TiO_2 elicited most severe inflammatory reactions. Further, coated TiO_2 particles induced bronchoalveolar lavage fluid (BALF) cell DNA damage, whereas uncoated particles revealed no apparent effects. Ruenraroengsak and coworkers (2012) described the impact of unprocessed and surface-modified polystyrene latex nanoparticles (NP; 50 and 100 nm) on transformed human alveolar epithelial type 1-like cells. Data demonstrated less severe membrane damage and reactivity using unprocessed particles and carboxyl modifications compared to amine-modified polystyrene NP, which generate excessive cell membrane damage.

The first aim of this study was to examine CBNP surface modifications. For this, Printex®90 covered with about 15% by weight of benzo[a]pyrene or 9-nitroanthracene (BaP-Pr90, NA-Pr90) and acetylene carbon black containing approximately 20% by weight polycyclic aromatic hydrocarbons (PAH-AB) were applied in doses of 7 μg each by oropharyngeal aspiration to mice. It is postulated that all CBNP surfaces affect the terminal respiratory tract, but it is unclear which surface modification exhibits the highest potential.

Because proteins may cover or modify CBNP surfaces and thus change their mode of action, the second aim was to determine the toxic potential of the vehicle composition using a dose of 7 μg unmodified Printex®90 suspended with or without bovine serum albumin ($Pr90^{+/-BSA}$).

Type II pneumocytes represent approximately 7% of the alveolar region; however, these are one of the most metabolic active cell types in the gas exchange region. Type II pneumocytes produce pulmonary surfactant and replace type I cells in repair processes (Adamson and Bowden, 1975; Crapo et al., 1982; Wright and Hawgood, 1989; Gumbleton, 2001). With regard to their importance for lung integrity, these cells are the focus of our investigation. It is important to examine how CBNP surface modifications as well as particle suspension media play a role in interaction of NP with the terminal respiratory tract, especially type II pneumocytes.

Material and methods

Mice

Pathogen-free, 6- to 10-wk-old (18.6 ± 0.1 g), female BALB/*c* mice (Charles River Laboratories, Sulzfeld, Germany) were used for all experiments. Before oropharyngeal aspirations, mice acclimatized for 1 wk. All experiments complied with German legislation for animal studies and were conducted under the approval of the local authorities (Regional Council Giessen).

Particles

Spherical-shaped primary CBNP used in this study were Printex®90, kindly supplied by Evonik Industries (Hanau, Germany). The surface of Printex®90 CBNP was modified by covering with the polycyclic aromatic hydrocarbon benzo[a]pyrene (Alfa Aesar GmbH & Co KG, Karlsruhe, Germany) or 9-nitroanthracene (Merck Schuchardt OHG, Hohenbrunn, Germany). For this purpose, the respective amounts of CBNP and benzo[a]pyrene or 9-nitroanthracene were suspended with an ultrasonic finger in diethyl ether (Merck KGaA, Darmstadt, Germany). After this the solvent was removed at room temperature (RT). The coverage of the CBNP with benzo[a]pyrene or 9-nitroanthracene amounted to about 15% by weight. Acetylene carbon black was synthesized by gas phase synthesis in a low-pressure flat flame burner. Synthesis was carried out with an acetylene/oxygen ratio of 1.1:1 at a pressure of 70 mbar. The acetylene carbon black contained approximately 20% by weight of a polycyclic aromatic hydrocarbon (PAH) mixture. Crystalline silica DQ12 reference particles were obtained from Bergbauforschung Essen (Germany).

The samples were characterized by different methods. The mass loss at 1000 °C in inert conditions was measured by thermogravimetry (DuPont Instruments 951 Thermogravimetric Analyzer, Wilmington, DE) and is primarily due to desorbing PAH, benzo[a]pyrene or 9-nitroanthracene. In addition, absorbed gases (oxygen, nitrogen) may be released or degradation reactions may occur. The primary particle diameter was determined by scanning electron microscopy (Leo 1530,

Oberkochen, Germany). The mean diameter was determined only for unmodified Printex®90 and acetylene CB without PAH. Scanning electron microscope images were used to determine mean particle diameters. Already during image acquisition Printex®90 modified with BaP or NA resulted in massive aggregation and agglomeration, which avoided accurate measurements. A log-normal size distribution was fitted to the measured particle size distribution to determine the average particle diameter and standard deviation. The specific surface area was measured by Brunauer–Emmett–Teller analysis (BET) with nitrogen (Bel Japan Inc. Belsorp Mini 2, Osaka, Japan), the particle size in medium by dynamic light scattering, and zeta potential in medium by zeta potential measurements (Malvern ZetaSizer Nano ZS, Herrenberg, Germany). The results and the abbreviations used in this article are given in Table 1. During all exposure experiments, size distributions were monitored using a ZetaSizer Nano ZS by the Fraunhofer ITEM Hannover. In addition, all particles were examined for endotoxin using the Chromo-LAL test (Associates of Cape Cod, Inc., East Falmouth, MA) to eliminate contaminations in particle suspensions.

The PAH on the acetylene CB were identified by gas chromatography–mass spectrometry (Shimadzu GCMS-QP2010 SE, Kyoto, Japan). The main component is acenaphthylene. Further, higher amounts of biphenyl, fluorene, phenanthrene, 4*H*-cyclopenta[def]phenanthrene, anthracene, fluoranthene and cyclopenta[cd]pyrene, or benzo[ghi]fluoranthene were detected. All surface-modified CBNP were suspended using distilled water containing 0.5% BSA Fraction 5 (Pan-Biotech GmbH, Aidenbach, Germany), because saline as well as distilled water alone did not result in nanoscaled particle suspensions. Only unmodified Printex®90 was adequately suspendable in distilled water with no additives ($Pr90^{-BSA}$). Thus, the importance of the protein coating could be tested. DQ12 quartz suspended in distilled water (DQ12), saline (NaCl), and distilled water with and without 0.5% BSA ($H_2O^{+/-BSA}$) were used as reference particle and negative controls.

Exposure protocol

Mice were anesthesized with Isofluran (Baxter AG, München, Germany) to apply single-particle

Table 1. Particle Characteristics

Particle dose (µg/70 µl)	Particle/ controls	Surface functionalization	Distilled water (vehicle) ± 0.5% BSA	Primary mean particle diameter (nm)	Mass loss at 1000°C (%)	Specific surface area (m^2/g)	*Z*-average (nm)	Zeta potential (mV)	Abbreviation
7	Printex®90	–	–	16.5 ± 0.4 (0.3 ± 0.0)	0.5 ± 0.4	302 ± 16	126.7 ± 1.2	+35.7 ± 1.2	$Pr90^{-BSA}$
7	Printex®90	–	+	16.5 ± 0.4 (0.3 ± 0.0)	0.5 ± 0.4	302 ± 16	153.8 ± 1.2	−30.8 ± 1.3	$Pr90^{+BSA}$
7	Printex®90	9-Nitroanthracene	+	No measurements	16.1 ± 0.5	91 ± 0	169.0 ± 2.0	−31.0 ± 1.0	NA-Pr90
7	Printex®90	Benzo[a]pyrene	+	No measurements	14.6 ± 0.1	91 ± 2	172.1 ± 2.6	−34.8 ± 2.9	BaP-Pr90
7	Acetylene Carbon black	Polycyclic aromatic hydrocarbons	+	14.2 ± 0.1 (0.1 ± 0.0)*	19.0 ± 0.7	115 ± 3	177.6 ± 0.6	−34.4 ± 1.4	PAH-AB
7	DQ12 quartz	–	–	1300	–	1.5	No measurements		DQ12
0	0.9% saline	–	–	–	–	–	–	–	NaCl
0	Distilled water	–	–	–	–	–	–	–	H_2O^{-BSA}
0	Distilled water	–	+	–	–	–	–	–	H_2O^{+BSA}

Note. Mean diameter was analyzed by scanning electron microscopy. Asterisk indicates measurement without PAH. The SDs of the lognormal distributions are illustrated in parentheses. The mass loss at 1000°C was determined by thermogravimetry. Surface area was calculated by the Brunauer–Emmett–Teller analysis (BET) with nitrogen. *Z*-average and zeta potential were measured by a Malvern ZetaSizer Nano ZS. Data are presented as arithmetic mean ± SD.

suspensions of 70 µl containing 7 µg particles via oropharyngeal aspiration. Dosages of 7 µg have been chosen on the basis of previous dose-response studies, for example, the study done by Stoeger and colleagues (2006). Low doses enable the detection of CBNP surface modification-induced effects, whereas surface area or lung overload exerted no marked impact. Control mice were handled similarly but obtained 0.9% saline, distilled water with or without 0.5% BSA (negative controls), or DQ12 quartz without BSA (reference particle), respectively. Lung function was determined 2 d postexposure. On d 3 mice were sacrificed to carry out bronchoalveolar lavage, type II pneumocyte isolation, and to receive lungs for histological examinations.

Head-out body plethysmography

Lung function (n = 5–20), measured as mid-expiratory flow rates (EF_{50}), was assessed using head-out body plethysmography (Hugo Sachs Elektronik-Harvard Apparatus GmbH, March-Hugstetten, Germany) 2 d postexposure. In brief, mice were exposed to acetyl-β-methylcholine chloride (MCh; Sigma Aldrich®, Steinheim, Germany) free air to acclimatize and record baseline values. Then a constant rising MCh gradient up to 125 mg MCh/ml phosphate-buffered saline (PBS; PAA-Laboratories GmbH, Pasching, Austria) was added. A tidal volume reduced to 50% marked the end of the measurement.

Lung fixation/histopathology

For histological examinations two nonlavaged lungs per group were removed as described earlier (Schreiber et al., 2013). Preliminary tests using similar CBNP concentrations showed only marginal effects on lung structures. For this reason, only two mice per group were used for histopathology. Briefly, mice were sacrificed with an ip injection of sodium pentobarbital (0.4 g/kg body weight/Heparin-Natrium) 25000-Ratiopharm (200 IU per mouse) mixture (Narcoren, Merial GmbH, Hallbergmoos, Germany; Ratiopharm GmbH, Ulm, Germany). Then lungs were instilled with 0.7 ml 3.5% neutral-buffered formalin (Otto Fischar GmbH & Co. KG, Saarbrücken, Germany) via trachea. Finally lungs were excised for embedding in paraffin and to prepare sections with a Leica SM R2000 microtome (Leica Microsystems Nussloch GmbH, Nussloch, Germany). Picrosirius red staining was used as overview staining and to demonstrate a possible beginning of collagen formation (Junqueira et al., 1979). This slight overview staining allows an easier detection of CBNP in lung tissue compared to HE staining. Immunohistological analysis of the antioxidant enzyme GPX 3 (1:500 dilution; LifeSpan Biosciences, Inc., Seattle, WA, catalogue number LS-C94195) and cell proliferation (Ki-67, 1:50 dilution; Abcam plc, Cambridge, UK, catalogue number ab15580) was conducted according to Schreiber et al. (2013).

Bronchoalveolar lavage fluid and type II pneumocyte isolation

Bronchoalveolar lavage fluid (BALF) and type II pneumocyte isolation (n = 6–20) was undertaken according to Corti et al. (1996). Modifications and detailed information were described previously (Schreiber et al., 2013). Briefly, mice were euthanized as described in the preceding. Then a cannula was fixed into the trachea to perform bronchoalveolar lavage and apply Dispase I solution (<2.44 U/ml PBS; Roche Diagnostic GmbH, Mannheim, Germany) and low-melt agarose (FMC BioProducts, Philadelphia, PA) for cell isolation following lung perfundation. After incubation in Dispase I solution (45 min, RT), lungs were transferred to 1.5 ml modified Dulbecco's modified Eagle's medium (DMEM) low glucose medium (18 mM glucose, 2 mM L-glutamine, 25 mM HEPES; PAA Laboratories, Pasching, Austria; Merck, Darmstadt, Germany; Sigma Aldrich, Steinheim, Germany) with 375 µg DNAse I (Roche Diagnostic, Mannheim, Germany) and cut with scissors to prepare lung homogenate. Subsequently, suspensions were filtered, centrifuged (10 min, 150 × g at 4 °C), and resuspended in 10 ml culture medium containing 10% fetal calf serum and 1% penicillin/streptomycin mixture (PAA Laboratories, Austria). Then type II pneumocyte isolation was carried out using petri dishes coated with anti-mouse CD45 (42 µg; BD Bioscience, Heidelberg, Germany) and anti-

mouse CD16/32 (16 µg; BD Bioscience, Heidelberg, Germany). After incubation (2 h, 37 °C, 10% CO_2 concentration), intact type II pneumocytes were counted via trypan blue staining (0.4%; Invitrogen LAB-SA Detection System, Invitrogen Corporation, USA). Finally, type II pneumocytes were resuspended in Isol-RNA Lysis reagent (5 Prime, Hamburg, Germany) and frozen at –80 °C until RNA isolation.

Lavage cell profile and biochemical analysis

Bronchoalveolar lavage fluid cell compositions (n = 6–20) were examined counting five representative microscope sections of cytocentrifuged cell preparations. Briefly, BALF was centrifuged (150 × g for 10 min at 4 °C), resuspended with 0.5 ml 0.9% saline, and transferred to a cytocentrifuge (40 × g for 15 min at RT; Shandon, Cytospin2, Block Scientific, New York, NY). Finally, cells were stained with the May–Grünwald Giemsa method (Microscopy, Giemsas Azur-Eosin-Methylenblau-Solution and May-Grünwalds Eosin-Methylenblau-Solution modified, Merck, Darmstadt, Germany). Aliquots of cell-free BALF (n = 6–20) were stored at –80 °C until total protein, phospholipid, and lactate dehydrogenase (LDH) levels were assessed using the BCA protein assay kit (Pierce, Rockford, USA), phospholipid measurement as described by Bartlett (1959), and lactate dehydrogenase activity assay (Roche Diagnostics, Mannheim, Germany).

Type II pneumocyte mRNA profile

Type II pneumocyte RNA purification and quantitative real-time reverse-transcription polymerase chain reaction analysis (qRT-PCR, n = 3–19) were conducted as described previously (Schreiber et al., 2013). In short, isolated cells were suspended in Isol-RNA Lysis Reagent (5 PRIME, Hamburg, Germany) and processed according to the recommended protocol. Total mRNA quantification was carried out by a Nano Drop1000 Spectrophotometer (peqlab, Erlangen, Germany). According to the manufacturer's instructions, RNA was converted by a cDNA Synthesis Kit (peqlab, Erlangen, Germany). qRT-PCR was performed using the Rotor-Gene SYBR Green PCR Kit and the Rotor-Gene Q (Qiagen, Hilden, Germany) according to the product manuals. Examinations focused on antioxidative enzymes, the cytokine interleukin (IL)-6, surfactant proteins, and enzymes of the surfactant synthesis. Sequences for the used primers are provided in Table 2. Fold changes were calculated using the ΔΔCt method (Livak and Schmittgen, 2001). Data are presented as fold change over H_2O^{-BSA} ± standard error of the mean (SEM).

Statistical analysis

Results and particle characteristics are expressed as arithmetic mean ± SEM and standard deviation (SD). Treatment-related differences were evaluated using the nonparametric Kruskal–Wallis and Mann–Whitney test. Those p values less than .05 were considered to be statistically significant.

Table 2. Primer Sequences and Sources

Genes	Primer forward 5`-3`	Primer reverse 5`-3`
Housekeeping gene		
RPL32[1]	Catalogue number QT01752387	
Antioxidative enzymes		
GR[2]	TCGGAATTCATGCACGATCAC	TGTTCAGGCGGCTCACATAG
GPX3[2]	AGGAAGCCACATTCCCAGTC	TGCCAAGCCGTAAACACAG
GPX4[2]	TCTCAGCCAAGGACATCGAC	CCAGGATTCGTAAACCACACTC
Catalase[1]	Catalogue number QT01058106	
Cytokine		
IL-6[2]	GGATACCACTCCCAACAGAC	CAATCAGAATTGCCATTGCAC
Surfactant proteins		
SP-A[2]	TCTTCTTGACTGTTGTTGCTG	TCTCCTTTGATACCATCTCTCC
SP-D[2]	ACAGCAACTCATCACAGCCC	TCTCCACACAGTTCTCTGCTC
Enzymes of the phospholipid synthesis		
CKα[2]	CAGCAACTGCACAAGATCC	ATAAGCATCAGCTTCCGCC
CKβ[2]	AACCTGCTCTTCCGATGCTCAC	TGCGAGAATGGCGAACATCAC
CTPα[2]	GAGCCTAACTTTTCTTACTCCC	CCACTCCTCTCTCCAATCAC

Note. Sources: 1, QIAGEN, Hilden, Germany; 2, Eurofins, Ebersberg, Germany.

Table 3. Lung Function and Type II Pneumocyte Cell Number and Protein Content

Experimental group	Lung function (%)	Isolated cells	Protein concentration per 1 million cells (µg/ml)
NaCl	67.7 ± 9.7†	$4.8 \times 10^6 \pm 4.8 \times 10^5$†	573.7 ± 75.8†
H_2O^{-BSA}	60.8 ± 6.0†	$6.4 \times 10^6 \pm 4.6 \times 10^5$†	482.9 ± 42.8†
H_2O^{+BSA}	41.1 ± 6.3	$6.4 \times 10^6 \pm 7.1 \times 10^5$	532.0 ± 46.1
$Pr90^{-BSA}$	71.1 ± 6.0†	$5.3 \times 10^6 \pm 5.0 \times 10^5$†	671.4 ± 73.5†
$Pr90^{+BSA}$	50.3 ± 6.2	$4.2 \times 10^6 \pm 4.5 \times 10^5$	726.9 ± 60.5
NA-Pr90	67.2 ± 4.6	$4.4 \times 10^6 \pm 3.1 \times 10^5$	925.9 ± 102.5*
BaP-Pr90	70.4 ± 11.1	$6.6 \times 10^6 \pm 8.1 \times 10^5$	591.4 ± 46.3
PAH-AB	36.7 ± 6.7*	$7.8 \times 10^6 \pm 4.8 \times 10^5$*	478.6 ± 34.5
DQ12	42.5 ± 5.2†	$7.4 \times 10^6 \pm 1.0 \times 10^6$†	375.1 ± 43.6†*

Note. Absolute values are demonstrated as arithmetic mean ± SEM (n = 6–20)
†Control and reference data from an earlier publication (Schreiber et al., 2013); Kruskal–Wallis and Mann–Whitney test.
*Significant changes compared to the NaCl control ($p < .05$).

Results

Lung function

Lung function was evaluated by measurement of airway hyperresponsiveness via noninvasive head-out body plethysmography (Table 3). Compared to saline control, exposure to PAH-AB induced a significant reduced pulmonary function. In contrast, $Pr90^{+BSA}$, the reference particle DQ12, and the H_2O^{+BSA} control initiated numerically decreased tidal midexpiratory flow rates, whereas H_2O^{-BSA}, $Pr90^{-BSA}$, NA-Pr90, and BaP-Pr90 produced no marked lung function alterations. Saline, H_2O^{-BSA}, DQ12, and $Pr90^{-BSA}$ reference data from lung function measurements as well as some of the following results were taken from our previous study to reduce the number of animal experiments (Schreiber et al., 2013).

Collagen structures, overview staining, cell proliferation, and antioxidant status

Often functional lung impairment is accompanied by structural alterations like formation of edema and fibrosis (Wang et al., 2010; Organ at al., 2015). Therefore, collagen structures were determined using picrosirius red staining. Neither collagen accumulations nor lung deformations such as thickened alveolar septa were noted in all exposure groups, but slight picrosirius red staining allowed CBNP detecting in lung tissues as seen in Figure 1.

Cell proliferation occurring during inflammation was detected using the proliferation marker Ki-67. H_2O^{+BSA}, DQ12, and PAH-AB exposure induced positive labeled bronchial epithelia, whereas $Pr90^{+BSA}$ and BaP-Pr90 revealed intensive staining of both bronchial epithelia and cells of the alveolar septa. NaCl, H_2O^{-BSA}, $Pr90^{-BSA}$, and NA-Pr90 treatment induced no marked changes in cell proliferation. Alterations of the antioxidant status were detected using GPX 3-stained tissues, demonstrating positive labeled bronchial epithelia and type II pneumocytes in all exposure groups.

Bronchoalveolar lavage fluid alterations

Both DQ12 and CBNP treatments failed to induce alterations in protein, phospholipid (Table 4), or LDH activity levels (data are not shown) in BALF compared to NaCl control. $Pr90^{-BSA}$ produced significant decreased cell yields attributed to a markedly diminished amount of macrophages compared to saline control. Neutrophil and eosinophil granulocytes remained unchanged throughout all CBNP-treated groups. The yield of lymphocytes fell significantly after exposure to $Pr90^{+BSA}$ and BaP-Pr90.

Type II pneumocyte cell number, protein content, and mRNA status

Cell count (Table 3) revealed a significant increased cell yield following application of PAH-AB compared to control. H_2O^{-BSA}, H_2O^{+BSA}, $Pr90^{-BSA}$, BaP-Pr90, and DQ12 produced a numerical rise in cell yield, whereas exposures with $Pr90^{+BSA}$ and NA-Pr90 induced no marked changes.

Type II pneumocyte cell protein measurements (Table 3) demonstrated a significant elevated concentration following NA-Pr90 aspiration and marked reduced level following DQ12 exposure

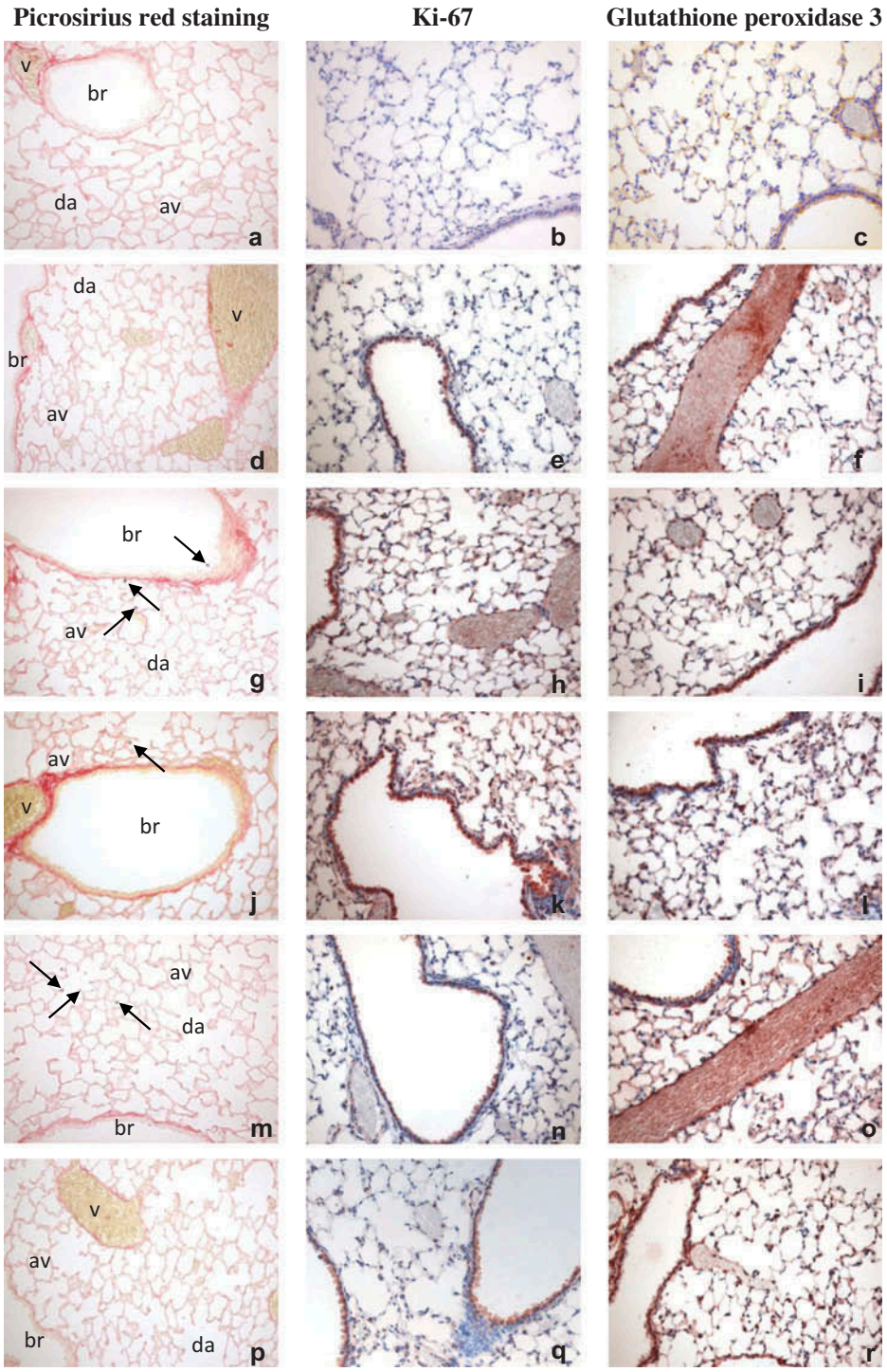

Figure 1. Representative picrosirius red (overview staining, collagen marker) and immunohistochemical stained lung tissues (proliferation marker Ki-67; antioxidant active enzyme glutathione peroxidase 3) from BALB/*c* mice. Exposure groups: NaCl (a–c); H_2O^{+BSA} (d–f); $Pr90^{+BSA}$ (g–i); BaP-Pr90 (j–l); PAH-AB (m–o); and DQ12 (p–r). Abbreviations: av, alveolus; b, bronchiolus; da, ductus alveolaris; v, blood vessel. Arrows indicate CBNP and collagen structures appear dark red. Positive Ki-67 and glutathione peroxidase 3 tissues appear brown. Light microscopic images were taken at ×200 magnification.

compared to control. H_2O^{-BSA}, H_2O^{+BSA}, and PAH-AB exposures numerically reduced protein concentration, whereas $Pr90^{-BSA}$, $Pr90^{+BSA}$, and BaP-Pr90 produced numerical increased levels.

Gene profiles of these cells such as antioxidative active enzymes (GR, GPX3, GPX4, and CAT), the cytokine IL-6, surfactant proteins (SP-A and SP-D), and enzymes of surfactant synthesis (CKα,

Table 4. Bronchoalveolar Lavage Fluid Parameters

Experimental group	Protein (µg/ml)	Phospholipid (µg/ml)	Cell yields	Macrophages	Neutrophils	Lymphocytes	Eosinophils
NaCl†	182.0 ± 24.3	94.1 ± 4.7	52.8 ± 4.9	51.5 ± 4.7	0.8 ± 0.3	0.5 ± 0.1	0.0 ± 0.0
H_2O^{-BSA}†	184.0 ± 14.3	109.7 ± 8.0	46.4 ± 3.5	44.7 ± 3.6	1.4 ± 0.5	0.2 ± 0.1	0.1 ± 0.1
H_2O^{+BSA}	175.6 ± 15.8	115.3 ± 7.5	56.7 ± 7.2	55.9 ± 7.3	0.7 ± 0.2	0.2 ± 0.1	0.1 ± 0.1
$Pr90^{-BSA}$†	205.7 ± 14.8	96.6 ± 9.4	39.4 ± 2.8*	37.7 ± 2.7*	0.8 ± 0.3	0.5 ± 0.1	0.4 ± 0.2
$Pr90^{+BSA}$	188.1 ± 22.8	75.2 ± 7.2	59.4 ± 7.8	58.8 ± 7.6	0.4 ± 0.2	0.1 ± 0.0*	0.2 ± 0.1
NA-Pr90	130.6 ± 26.2	102.5 ± 14.2	51.4 ± 5.7	51.1 ± 5.8	0.1 ± 0.1	0.2 ± 0.1	0.1 ± 0.1
BaP-Pr90	172.4 ± 24.1	98.3 ± 4.5	53.2 ± 4.7	52.6 ± 4.7	0.3 ± 0.1	0.1 ± 0.0*	0.1 ± 0.0
PAH-AB	206.5 ± 11.9	116.8 ± 11.8	70.6 ± 7.0	68.4 ± 6.9	1.9 ± 0.9	0.4 ± 0.1	0.2 ± 0.1
DQ12†	196.9 ± 14.7	96.4 ± 8.4	52.9 ± 6.7	51.0 ± 6.4	1.1 ± 0.3	0.5 ± 0.1	0.2 ± 0.1

Note. Bronchoalveolar lavage fluid parameters are demonstrated as arithmetic mean ± SEM (n = 6–20). Cell analysis was carried out by counting five representative panels per slide.
†Control and reference data from an earlier publication (Schreiber et al., 2013); Kruskal–Wallis and Mann–Whitney Test.
*Significantly reduced compared to the saline control ($p < .05$).

Table 5. Type II Pneumocyte mRNA Profile

Experimental group	GR	GPX3	GPX4	Catalase	IL-6	SP-A	SP-D	CKα	CKβ	CTPα
H_2O^{-BSA}	1.0 ± 0.1	1.0 ± 0.1†	1.0 ± 0.1	1.0 ± 0.1	1.0 ± 0.1†	1.0 ± 0.1	1.0 ± 0.0	1.0 ± 0.1	1.0 ± 0.1	1.0 ± 0.2
NaCl	0.7 ± 0.2	0.7 ± 0.1†	1.0 ± 0.3	0.8 ± 0.2	0.7 ± 0.2†	0.6 ± 0.3*	0.7 ± 0.1*	0.3 ± 0.1*	0.7 ± 0.2	0.7 ± 0.2
H_2O^{+BSA}	0.8 ± 0.1	0.6 ± 0.1	0.7 ± 0.1	1.0 ± 0.3	1.0 ± 0.3	0.8 ± 0.2	0.9 ± 0.1	0.5 ± 0.2*	0.6 ± 0.1	0.5 ± 0.1
$Pr90^{-BSA}$	1.2 ± 0.3	1.5 ± 0.2†	1.4 ± 0.3	0.8 ± 0.2	1.2 ± 0.3†	0.7 ± 0.1	0.8 ± 0.1*	0.9 ± 0.1	0.8 ± 0.1	1.1 ± 0.2
$Pr90^{+BSA}$	0.5 ± 0.1	1.2 ± 0.1	0.4 ± 0.1*	0.3 ± 0.1*	1.7 ± 0.4	0.9 ± 0.1	1.2 ± 0.2	0.5 ± 0.1*	0.6 ± 0.1	0.6 ± 0.1
NA-Pr90	1.1 ± 0.0	0.4 ± 0.1*	1.3 ± 0.2	1.3 ± 0.1	1.4 ± 0.2	0.1 ± 0.0*	1.0 ± 0.2	0.3 ± 0.1*	0.5 ± 0.2	0.4 ± 0.2
BaP-Pr90	0.4 ± 0.1*	1.0 ± 0.2	0.7 ± 0.1	0.9 ± 0.2	0.7 ± 0.1	1.0 ± 0.2	1.3 ± 0.1	1.2 ± 0.3	1.0 ± 0.2	0.7 ± 0.1
PAH-AB	0.6 ± 0.2	0.6 ± 0.1*	0.5 ± 0.2*	0.8 ± 0.2	1.1 ± 0.2	0.4 ± 0.1*	0.8 ± 0.1	0.3 ± 0.1*	0.6 ± 0.1	0.3 ± 0.1*
DQ12	0.6 ± 0.1	0.9 ± 0.2†	0.7 ± 0.2	0.4 ± 0.1*	1.3 ± 0.3†	0.2 ± 0.1*	0.6 ± 0.1*	0.3 ± 0.1*	0.3 ± 0.0*	0.2 ± 0.1*

Note. qRT-PCR results ($2^{-\Delta\Delta CT}$) are reported as fold change over H_2O^{-BSA} ± SEM (n = 3–19).
†Control and reference data from an earlier publication (Schreiber et al., 2013); Kruskal–Wallis and Mann–Whitney test.
*Significant reduced compared to the H_2O^{-BSA} control ($p < .05$).

CKβ and CTPα) were analyzed using qualitative real time RT-PCR (Table 5). $Pr90^{-BSA}$ induced a significant reduced SP-D mRNA expression, whereas $Pr90^{+BSA}$ produced markedly decreased GPX4, CAT, and CKα mRNA levels. NA-Pr90 significantly lowered GPX3, SP-A, and CKα mRNA expressions. Reduced GR mRNA levels were noted after BaP-Pr90 exposure. PAH-AB displayed diminished GPX3, GPX4, SP-A, CKα, and CTPα mRNA expressions, whereas DQ12 exposure produced reduced CAT, SP-A, SP-D, CKα, CKβ, and CTPα mRNA levels.

Discussion

Carbon black nanoparticles (CBNP) were found to alter the respiratory tract. In agreement with our findings, Niwa et al. (2008) observed in rats that inhaled CBNP resulted in minor inflammatory processes. Further, Bourdon and coworkers (2013) reported lung inflammation and genotoxicity in lungs, as well as in cells present in BAL.

Due to the different industrial requirements, CBNP parameters like particle structure or chemical composition were altered. This also includes the modification of the surface area with chemical components (Long et al., 2013). However, the influence of this particle characteristic and composition of suspension media on adverse lung effects has not thus far been studied. For this the acute 3 d mouse model was used in which CBNP were applied via oropharyngeal aspiration. This method represents a less complex experimental setup compared to inhalation exposures and guarantees a reliable particle distribution across the lungs (Rao et al., 2003; Lakatos et al., 2006). CBNP compared were Printex®90, surface-modified Printex®90 with benzo[a]pyrene (BaP-Pr90) or 9-nitroanthracene (NA-Pr90), and acetylene CB with polycyclic aromatic hydrocarbons (PAH-AB). Unmodified Printex®90 was suspended in distilled water with or without BSA ($Pr90^{+/-BSA}$).

Particle inhalation was shown to induce impairment of lung function and structural lung alterations (Anderson et al., 2011). Kamata and coworkers (2011) observed no altered lung mechanics using 10 μg CBNP at an exposure time of 21 d. Of all NP tested in this study, only PAH-AB induced restricted pulmonary function. However, the short-term experiment and low particle dose of all surface-modified test materials produced no marked alterations in lung epithelia, suggesting low toxic potential. This interpretation is in agreement with the observed low epithelial cell proliferation and unchanged expression of the antioxidant GPX3. Previous studies also reported no structural changes in lung tissues after low-dose CBNP applications (Kamata et al., 2011; Jackson et al., 2012). It is apparent that the particle dose used in these experiments was too low to produce severe damage or to elevate production of antioxidative enzymes above levels present in normal tissues (Kinnula and Crapo, 2003).

Previously, Schreiber et al. (2013) found a significant reduced cell yield in BALF after aspiration of 7 μg $Pr90^{-BSA}$ that is attributed to a reduced quantity of macrophages. In addition, lower lymphocyte levels after $Pr90^{+BSA}$ and BaP-Pr90 exposure were noted. Similar observations were reported by Roursgaard and colleagues (2011)

such that application of 5 μg DQ12 particles resulted in decreased macrophage levels in BAL. In agreement with their findings, this is due to migration of particle-laden macrophages from alveoli, which represents the main clearance process of inhaled substances in the alveolar region (Sibille and Reynolds, 1990). In contrast, a marked influx of lymphocytes, macrophages, and neutrophil and eosinophil granulocytes following IT instillation of 18 μg Printex®90 was noted by Bourdon and colleagues (2012). Possible reasons for these differences may be based on the use of different application methods (oropharyngeal aspiration vs. IT instillation) and amount of CBNP used (7 μg vs. 18 μg).

Results obtained from our experiments showed no marked changes in BALF protein, phospholipid, and LDH concentrations by any CBNP, indicating an intact lung. Unchanged protein concentrations in BALF were also seen by Kyjovska and colleagues (2015) 3 d after IT instillation of 6 μg Printex®90. However, photometric assays are susceptible especially to interactions between carbon particles and detection substances or to light absorption (Stone et al., 2009; Dhawan and Sharma, 2010). In addition, lung surfactant composed of lipids and proteins may interact with the surface of inhaled CBNP and change or abrogate their chemical modifications (Hamm et al., 1996; Dutta et al., 2007). It is also known that CBNP adsorb dipalmitoylphosphatidylcholine (DPPC), which contributes to particle agglomeration (Kendall et al., 2004). This may explain the appearance of CBNP agglomerates in macrophages from BAL and lung tissue.

The observed PAH-AB induced type II pneumocyte cell proliferation normally replace degenerated type I pneumocytes (Adamson and Bowden, 1975), but unchanged LDH concentrations in BALF contradict cell degeneration. An opposite observation is the elevated cell protein concentrations induced by 9-nitroanthracene modified Printex®90, whereas the aspirated DQ12 reference lowered cell protein. Hence, further in vivo and in vitro studies with modified CBNP are necessary to analyze their interaction with single surfactant components, as well as particle uptake mechanisms of alveolar cells.

From all surfactant proteins SP-A and SP-D are known to be part of the innate immune system, in which their main function is to bind to potential harmful substances to improve particle uptake by phagocytic cells (Wright, 1997). The observed partially reduced surfactant protein mRNA expression in type II pneumocytes is hard to explain since this contrasts with our expectations. Other studies focused on direct interactions between particles and hydrophilic proteins and its consequences but not on mRNA expression. Salvador-Morales and coworkers (2007) showed that carbon nanotubes bind SP-A and SP-D depending upon calcium concentration. In our study, CBNP surface modifications induced changes in surfactant protein, antioxidant, and surfactant synthesis enzyme mRNA expression, but none of the surfaces studied exhibited a marked effect.

In a subset of the experiment the influence of suspension media was tested using $Pr90^{-BSA}$ and $Pr90^{+BSA}$. Differences in lung functions, cell proliferation status, BAL cell compositions, type II pneumocyte cell yields, and mRNA expression all show that this and particle suspension media alter interactions of CBNP with cells of the terminal respiratory tract.

In summary, the hypothesis that chemical-modified CBNP and use of different suspension media influence CBNP lung cell interactions at least in part has been verified. Both particles and suspension media revealed no marked changes in lung structure, but type II pneumocyte metabolism was affected as seen by varying mRNA expression. Based on these results, future studies may be essential to obtain additional data on surface modified CBNP. Especially, long-term exposures with repeated NP applications and studies on predamaged lungs will help to classify the toxic potential of CBNP surface modifications.

Competing interests

All listed authors declare no competing interest.

Funding

The authors gratefully thank Thomas Ruppersberg of the Department of Clinical Chemistry/Central Laboratories of the Philipps University Marburg for his assistance during head-out body plethysmography and Werner Cassel for his support

during statistical analysis, as well as our project partners at the Fraunhofer ITEM Hannover for particle sample preparation and measurements. This work was funded by the German Ministry of Education and Research (BMBF; grant 03X0093B).

References

Adamson, I. Y. R., and Bowden, D. H. 1975. Derivation of type I epithelium from type II cells in the developing rat lung. *Lab. Invest*. 32: 736–745.

Anderson, J. O., Thundiyil, J. G., and Stolbach, A. 2011. Clearing the air: A review of the effects of particulate matter air pollution on human health. *J. Med. Toxicol*. 8: 166–175.

Bartlett, G. R. 1959. Phosphorus assay in column chromatography. *J. Biol. Chem*. 234: 466–468.

Bourdon, J. A., Saber, A. T., Jacobsen, N. R., Jensen, K. A., Madsen, A. M., Lamson, J. S., Wallin, H., Møller, P., Loft, S., Yauk, C. L., and Vogel, U. B. 2012. Carbon black nanoparticle instillation induces sustained inflammation and genotoxicity in mouse lung and liver. *Part. Fibre Toxicol*. 9: 5.

Bourdon, J. A., Williams, A., Kuo, B., Moffat, I., White, P. A., Halappanavar, S., Vogel, U., Wallin, H., and Yauk, C. L. 2013. Gene expression profiling to identify potentially relevant disease outcomes and support human health risk assessment for carbon black nanoparticle exposure. *Toxicology* 303: 83–93.

Ceresana, Market Intelligence, Consulting, 2014. Market study: Carbon BLack (UC-5605). http://www.ceresana.com/en/market-studies/chemicals/carbon-black/ceresana-market-study-carbon-black.html (accessed November 26, 2014).

Corti, M., Brody, A. R., and Harrison, J. H. 1996. Isolation and primary culture of murine alveolar type II cells. *Am J. Respir. Cell Mol. Biol*. 14: 309–315.

Crapo, J. D., Barry, B. E., Gehr, P., Bachofen, M., and Weibel, E. R. 1982. Cell number and cell characteristics of normal human lung. *Am. Rev. Respir. Dis*. 125: 332–337.

Dhawan, A., and Sharma, V. 2010. Toxicity assessment of nanomaterials: Methods and challenges. *Anal. Bioanal. Chem*. 398: 589–605.

Dumortier, H., Lacotte, S., Pastorin, G., Marega, R., Wu, W., Bonifazi, D., Briand, J. P., Prato, M., Muller, S., and Bianco, A. 2006. Functionalized carbon nanotubes are non-cytotoxic and preserve the functionality of primary immune cells. *Nano Lett*. 6: 1522–1528.

Dutta, D., Sundaram, S. K., Teeguarden, J. G., Riley, B. J., Fifield, L. S., Jacobs, J. M., Addleman, S. R., Kaysen, G. A., Moudgil, B. M., and Weber, T. J. 2007. Adsorbed proteins influence the biological activity and molecular targeting of nanomaterials. *Toxicol. Sci*. 100: 303–315.

Gumbleton, M. 2001. Caveolae as potential macromolecule trafficking compartments within alveolar epithelium. *Adv. Drug Deliv. Rev*. 49: 281–300.

Hamm, H., Kroegel, C., and Hohlfeld, J. 1996. Surfactant: A review of its functions and relevance in adult respiratory disorders. *Respir. Med*. 90: 251–270.

Han, S. G., Howatt, D., Daugherty, A., and Gairola, G. 2015. Pulmonary and atherogenic effects of multi-walled carbon nanotubes (MWCNT) in apolipoprotein-E-deficient mice. *J. Toxicol. Environ. Health A* 78: 244–253.

International Agency for Research on Cancer/World Health Organization. 2010. Carbon black, titanium dioxide, and talc. *IARC Monogr. Eval. Carcinogen. Risks Hum*. 93. http://monographs.iarc.fr/ENG/Monographs/vol93 (accessed September 16, 2014).

Jackson, P., Hougaard, K. S., Vogel, U., Wu, D., Casavant, L., Williams, A., Wade, M., Yauk, C. L., Wallin, H., and Halappanavar, S. 2012. Exposure of pregnant mice to carbon black by intratracheal instillation: Toxicogenomic effects in dams and offspring. *Mutat. Res*. 745: 73–83.

Junqueira, L. C., Bignolas, G., and Brentani, R. R. 1979. Picrosirius staining plus polarization microscopy, a specific method for collagen detection in tissue sections. *Histochem. J*. 11: 447–455.

Kamata, H., Tasaka, S., Inoue, K., Miyamoto, K., Nakano, Y., Shinoda, H., Kimizuka, Y., Fujiwara, H., Ishii, M., Hasegawa, N., Takamiya, R., Fujishima, S., Takano, H., and Ishizaka, A. 2011. Carbon black nanoparticles enhance bleomycin-induced lung inflammatory and fibrotic changes in mice. *Exp. Biol. Med*. 236: 315–324.

Kendall, M., Brown, L., and Trought, K. 2004. Molecular adsorption at particle surfaces: A PM toxicity mediation mechanism. *Inhal. Toxicol*. 16: 99–105.

Kim, H., Oh, S. J., Kwak, H. C., Kim J. K., Lim, C. H., Yang, J. S., Park, K., Kim, S. K., and Lee, M. Y. 2012. The impact of intratracheally instilled carbon black on the cardiovascular system of rats: elevation of blood homocysteine and hyperactivity of platelets. *J. Toxicol. Environ. Health A* 75: 1471–1483.

Kinnula V. L., and Crapo, J. D. 2003. Superoxide dismutases in the lung and human lung diseases. *Am. J. Respir. Crit. Care Med*. 167: 1600–1619.

Kyjovska, Z. O., Jacobsen, N. R., Saber, A. T., Bengtson, S., Jackson, P., Wallin, H., and Vogel, U. 2015. DNA damage following pulmonary exposure by instillation to low doses of carbon black (Printex®90) nanoparticles in mice. *Environ. Mol. Mutagen*. 56: 41–49.

Lakatos, H. F., Burgess, H. A., Thatcher, T. H., Redonnet, M. R., Hernady, E., Williams, J. P., and Sime, P. J. 2006. Oropharyngeal aspiration of a silica suspension produces a superior model of silicosis in the mouse when compared to intratracheal instillation. *Exp. Lung Res*. 32: 181–199.

Livak, K. J., and Schmittgen, T. D. 2001. Analysis of relative gene expression data using real-time quantitative PCR and the 2(–delta delta C(T)) method. *Methods* 25: 402–408.

Long, C. M., Nascarella, M. A., and Valberg, P. A. 2013. Carbon black vs. black carbon and other airborne materials containing elemental carbon: Physical and chemical distinctions. *Environ. Pollut*. 181: 271–286.

Nassimi, M., Schleh, C., Lauenstein, H. D., Hussein, R., Hoymann, H. G., Koch, W., Pohlmann, G., Krug, N., Sewald, K., Rittinghausen, S., Braun, A., and Müller-Goymann, C. 2010. A toxicological evaluation of inhaled solid lipid nanoparticles used as a potential drug delivery system for the lung. *Eur. J. Pharm. Biopharm*. 75: 107–116.

Niwa, Y., Hiura, Y., Sawamura, H., and Iwai, N. 2008. Inhalation exposure to carbon black induces inflammatory response in rats. *Circ. J*. 72: 144–149.

Organ, L., Bacci, B., Koumoundouros, E., Barcham, G., Milne, M., Kimpton, W., Samuel, C., and Snibson, K. 2015. Structural and functional correlations in a large animal model of bleomycin-induced pulmonary fibrosis. *Pulmon. Med*. 15: 81.

Rao, G. V., Tinkle, S., Weissman, D. N., Antonini, J. M., Kashon, M. L., Salmen, R., Battelli, L. A., Willard, P. A., Hoover, M. D., and Hubbs, A. F. 2003. Efficacy of a technique for exposing the mouse lung to particles aspirated from the pharynx. *J. Toxicol. Environ. Health A* 66: 1441–1452.

Renwick, L. C., Brown, D., Clouter, A., and Donaldson, K. 2004. Increased inflammation and altered macrophage chemotactic responses caused by two ultrafine particle types. *Occup. Environ. Med*. 61: 442–447.

Roursgaard, M., Jensen, K. A., Poulsen, S. S., Jensen, N. E., Poulsen, L. K., Hammer, M., Nielsen, G. D., and Larsen, S. T. 2011. Acute and subchronic airway inflammation after intratracheal instillation of quartz and titanium dioxide agglomerates in mice. *Sci. World J*. 11: 801–825.

Ruenraroengsak, P., Novak, P., Berhanu, D., Thorley, A. J., Valsami-Jones, E., Gorelik, J., Korchev, Y. E., and Tetley, T. D. 2012. Respiratory epithelial cytotoxicity and membrane damage (holes) caused by amine-modified nanoparticles. *Nanotoxicology* 6: 94–108.

Saber, A. T., Jensen, K. A., Jacobsen, N. R., Birkedal, R., Mikkelsen, L., Møller, P., Loft, S., Wallin, H., and Vogel, U. 2012. Inflammatory and genotoxic effects of nanoparticles designed for inclusion in paints and lacquers. *Nanotoxicology*. 6: 453–471.

Saber, A. T., Lamson, J. S., Jacobsen, N. R., Ravn-Haren, G., Hougaard, K. S., Nyendi, A. N., Wahlberg, P., Madsen, A. M., Jackson, P., Wallin, H., and Vogel, U. 2013. Particle-induced pulmonary acute phase response correlates with neutrophil influx linking inhaled particles and cardiovascular risk. *PLoS ONE* 8: e69020.

Salvador-Morales, C., Townsend, P., Flahaut, E., Vénien-Bryan, C., Vlandes, A., Green, M. L. H., and Sim, R. B. 2007. Binding of pulmonary surfactant proteins to carbon nanotubes: Potential for damage to lung immune defense mechanisms. *Carbon* 45: 607–617.

Sayes, C. M., Liang, F., Hudson, J. L., Mendez, J., Guo, W., Beach, J. M., Moore, V. C., Doyle, C. D., West, J. L., Billups, W. E., Ausman, K. D., and Colvin, V. L. 2006. Functionalization density dependence of single-walled carbon nanotubes cytotoxicity in vitro. *Toxicol. Lett*. 161: 135–142.

Schreiber, N., Ströbele, M., Kopf, J., Hochscheid, R., Kotte, E., Weber, P., Hansen, T., Bockhorn, H., and Müller, B. 2013. Lung alterations following single or multiple low-dose carbon black nanoparticle aspirations in mice. *J. Toxicol. Environ. Health A* 76: 1317–1332.

Shimada, A., Kawamura, N., Okajima, M., Kaewamatawong, T., Inoue, H., and Morita, T. 2006. Translocation pathway of the intratracheally instilled ultrafine particles from the lung into the blood circulation in the mouse. *Toxicol. Pathol*. 34: 949–957.

Sibille, Y., and Reynolds, H. Y. 1990. Macrophages and polymorphonuclear neutrophils in lung defense and injury. *Am. Rev. Respir. Dis*. 141: 471–501.

Stoeger, T., Reinhard, C., Takenaka, S., Schroeppel, A., Karg, E., Ritter, B., Heyder, J., and Schulz, H. 2006. Instillation of six different ultrafine carbon particles indicates a surface area threshold dose for acute lung inflammation in mice. *Environ. Health Perspect*. 114: 328–333.

Stone, V., Johnston, H., and Schins, R. P. F. 2009. Development of *in vitro* systems for nanotoxicology: Methodological considerations. *Crit. Rev. Toxicol*. 39: 613–626.

Wang, L., Mercer, R. R., Rojanasakul, Y., Qiu, A., Lu, Y. Scabilloni, J. F., Wu, N., and Castranova, V. 2010. Direct fibrogenic effects of dispersed single-walled carbon nanotubes on human lung fibroblasts. *J. Toxicol. Environ. Health A* 73: 410–422.

Wright, J. R. 1997. Immunomodulatory functions of surfactant. *Physiol. Rev*. 77: 931–962.

Wright, J. R., and Hawgood, S. 1989. Pulmonary surfactant metabolism. *Clin. Chest. Med*. 10: 83–93.

Yu, K. N., Kim, J. E., Seo, H. W., Chae, C., and Cho, M. H. 2013. Differential toxic responses between pristine and functionalized multiwall nanotubes involve induction of autography accumulation in murine lung. *J. Toxicol. Environ. Health A* 76: 1282–1292.